

Journal of Materials Chemistry C

Accepted Manuscript



This article can be cited before page numbers have been issued, to do this please use: S. Yang, M. Chu and Q. Miao, *J. Mater. Chem. C*, 2017, DOI: 10.1039/C7TC04092J.



This is an Accepted Manuscript, which has been through the Royal Society of Chemistry peer review process and has been accepted for publication.

Accepted Manuscripts are published online shortly after acceptance, before technical editing, formatting and proof reading. Using this free service, authors can make their results available to the community, in citable form, before we publish the edited article. We will replace this Accepted Manuscript with the edited and formatted Advance Article as soon as it is available.

You can find more information about Accepted Manuscripts in the [author guidelines](#).

Please note that technical editing may introduce minor changes to the text and/or graphics, which may alter content. The journal's standard [Terms & Conditions](#) and the ethical guidelines, outlined in our [author and reviewer resource centre](#), still apply. In no event shall the Royal Society of Chemistry be held responsible for any errors or omissions in this Accepted Manuscript or any consequences arising from the use of any information it contains.



Journal Name

ARTICLE

Connecting Two Phenazines with a Four-Membered Ring: Synthesis, Properties and Applications of Cyclobuta[1,2-b:3,4-b']diphenazines

Received 00th January 20xx,
Accepted 00th January 20xx

DOI: 10.1039/x0xx00000x

www.rsc.org/

Shuaijun Yang,^a Ming Chu^a and Qian Miao^{* a,b}

Herein we report cyclobuta[1,2-b:3,4-b']diphenazine (CBDP), a new π -electron molecular scaffold containing two phenazine moieties connected by a four-membered ring. With properly positioned silylethynyl substituting groups, CBDP offers a chromophore with large molar extinction coefficient, a luminophore with good quantum yield, and an n-type organic semiconductor with field effect mobility as high as 0.30 cm²/Vs. These properties are not available with the phenazine reference compounds, but can be tuned by adjusting the substituting positions of silylethynyl groups. On the basis of single crystal structures, UV-vis absorption and DFT calculation, it is concluded that the two phenazine subunits in CBDP are poorly conjugated in the ground state but strongly conjugated in the excited state, shedding light on the role of the four-membered ring in conjugation.

Introduction

Combining benzenoid and cyclobutadienoid rings in one polycyclic framework leads to interesting π -electron molecular scaffolds, whose electronic structures are governed by both aromaticity and antiaromaticity^{1, 2, 3, 4}. Herein we report cyclobuta[1,2-b:3,4-b']diphenazine (CBDP), a new π -electron molecular scaffold having two phenazine moieties connected by a four-membered ring. The linear π -backbone of CBDP is closely related to N-heteroacenes, which have recently been revived by the development of new synthetic methodology and the discovery of high-mobility n-type organic semiconductors⁵ based on N-heteroacenes.^{6, 7} Having N atoms replacing the CH units in the linear framework of acenes, N-heteroacenes are similar to acenes becoming less stable as their length increases. Such instability is an obstacle to development of larger N-heteroacenes for organic semiconductors or molecular wires with enhanced spatial electronic delocalization. To meet this challenge, N-heteroacenes were very recently extended through four-membered rings, which increase the length of N-heteroacenes without compromising their stability or changing their linear shape.^{8, 9, 10} The resultant π -extended N-heteroacenes, such as **1a**⁹ and **1b**¹⁰ as shown in Fig. 1a, are more stable than the

corresponding N-heteroacenes containing the same number of six-membered rings because insertion of formally antiaromatic

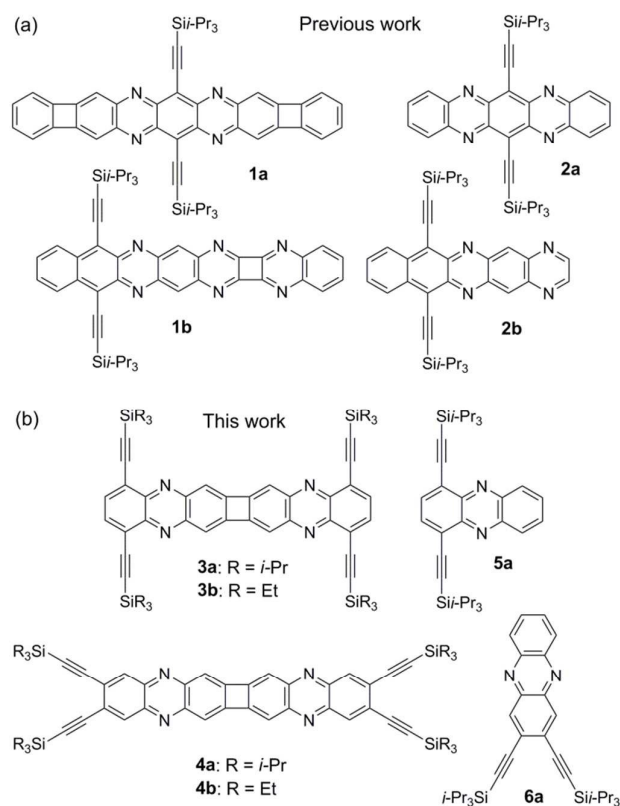


Fig. 1 (a) Structures of reported π -extended N-heteroacenes containing a four-membered ring and the corresponding N-heteroacenes; (b) structures of CBDPs and the related phenazines.

^aDepartment of Chemistry The Chinese University of Hong Kong, Shatin, New Territories, Hong Kong, China. E-mail: miaoqian@cuhk.edu.hk.

^bInstitute of Molecular Functional Materials (Areas of Excellence Scheme, University Grants Committee), Hong Kong, China.

† We dedicate this paper to Prof. Fred Wudl in celebrating 50 years of his contributions to the field of organic semiconductors.

Electronic Supplementary Information (ESI) available: Details of synthesis and characterization, DFT calculation, fabrication and characterization of organic thin film transistors, NMR spectra, See DOI: 10.1039/x0xx00000x

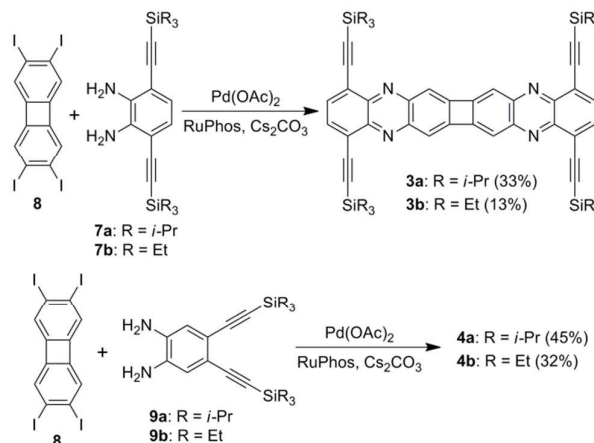
four-membered rings in fact increases the number of Clar's aromatic sextets. However, **1a** and **1b** both met problems in becoming high-mobility n-type semiconductors. **1a** is a poorer electron acceptor than the corresponding N-heteroacene **2a** with its lowest unoccupied molecular orbital (LUMO) energy level higher than that of **2a** by 0.33 eV. Although **1b** has a LUMO energy level lower than that of **2b** by 0.20 eV, the thin films of **1b** exhibited electron mobility ($0.015 \text{ cm}^2/\text{Vs}$) lower than that of **2b** by one order of magnitude presumably due to the poor crystallinity of the films as a result of the non-central symmetry of **1b**. To solve these problems, we became interested in linearly fused N-hetero polyarenes that differentiate themselves from **1a–b** by having two identical N-heteroacene units connected by a four membered ring. Detailed below are synthesis, properties and applications of silylethynylated CBDPs **3a–b** and **4a–b**, whose heptacyclic backbone, as shown in Fig. 1b, can be regarded as a unique dimer of phenazine with a four-membered carbocycle bridging the two monomers. In order to better understand the effect of the four-membered bridge in π -extension of N-heteroacenes, **3a–b** and **4a–b** were experimentally and computationally studied in comparison to the corresponding phenazine monomers, **5a** and **6a** (Fig. 1b), respectively. As found from the study detailed below, CBDP offers interesting optical and electronic properties that can be tuned by adjusting the substituting positions of silylethynyl groups but are not offered by the phenazine reference compounds, leading to solution-processed n-type semiconductors with field effect mobility of up to $0.30 \text{ cm}^2/\text{Vs}$.

Results and discussion

Synthesis

As shown in Scheme 1, CBDPs **3a–b** were synthesized by the Buchwald–Hartwig cross coupling¹¹ of the corresponding phenylenediamine **7a–b**¹² with 2,3,6,7-tetraiodobiphenylene (**8**), which was prepared from biphenylene by modifying the reported procedures.¹³ In the same way, compounds **4a–b** were synthesized from **8** and the corresponding phenylenediamines **9a–b**, which were prepared from 1,2-diiodo-4,5-dinitrobenzene¹⁴ in two steps following the reported procedures with minor modification.¹⁵ Unlike the reported synthesis of **1b**,¹⁰ the above coupling reactions did not yield N,N'-dihydro derivatives, which are expected as the products of the Buchwald–Hartwig cross coupling. This can be attributed to the spontaneous oxidation of the N,N'-dihydro derivatives to the final products in agreement with the fact that N,N'-dihydrophenazine is highly sensitive toward oxidation.¹⁶ Phenazine **5a** is a known compound as prepared by following the reported procedures,¹⁷ while **6a** was synthesized by the condensation reaction of *o*-benzoquinone and 4,5-dibromo-1,2-benzenediamine and the subsequent Sonogashira coupling as detailed in ESI. CBDPs **3a–b** and **4a–b** all exhibited good stability toward heating as well as ambient air and light (Fig. S1–S3 in ESI†). As found from differential

scanning calorimetry (DSC), **3a** and **4a** decomposed at $422 \text{ }^\circ\text{C}$ and $394 \text{ }^\circ\text{C}$, respectively, while heating the solids of **3a–b** and **4a–b** in air at $200 \text{ }^\circ\text{C}$ for four hours did not lead to detectable change in ^1H NMR spectra.



Scheme 1. Synthesis of **3a–b** and **4a–b**.

Crystal structures

Single crystals of **3b**, **4a** and **6a** suitable for X-ray crystallographic analysis were obtained in this study from their solutions by slow evaporation of solvents.¹⁸ The crystal structure of **5a**, as reported by Bunz et. al,¹⁹ contains two crystallographically independent molecules with slightly different bond lengths. The following discussion about bond lengths of **5a** refers to only one crystallographically independent molecule. Fig. 2a shows the π -backbones of **3b** and **4a** in comparison to those of **5a** and **6a**. In the crystals, the heptacyclic framework of **3b** is essentially flat, while that of **4a** is slightly bent along the long molecular axis as shown in Fig. 2b. As summarized in Table 1, the central four-membered rings in **3b** and **4a** have similar bond lengths: 1.49 \AA for C7–C8' and C7'–C8, and $1.43\text{--}1.44 \text{ \AA}$ for C7–C8 and C7'–C8'. The C7–C8' and C7'–C8 bonds in **3b** and **4a** are slightly shorter than the corresponding bonds in biphenylene (1.51 \AA),²⁰ but still slightly longer than typical nonconjugated single bonds between two sp^2 -hybridized C atoms ($1.47\text{--}1.48 \text{ \AA}$),²¹ suggesting absence of π character in these two bonds. The four-membered rings in **3b** and **4a** are bonded to four C atoms (C6, C9, C6' and C9') with C–C bond length ($1.34\text{--}1.35 \text{ \AA}$) very close to the typical bond length of C–C double bonds in alkenes ($1.31\text{--}1.34 \text{ \AA}$),²¹ suggesting a radialene-like structure. These bond lengths are in agreement with the earlier conclusion that the π bonds in [N]phenylenes tend to localize within the six-membered rings so that the 4π antiaromatic character of the cyclobutadiene linkage can be minimized.^{2,22} The C6–C7 and C8–C9 bonds in **3b** and **4a** are slightly shorter than the corresponding bonds in **5a** and **6a**, while the C5a–C6, C7–C8, C9–C9a and C5a–C9a bonds in **3b** and **4a** are slightly longer than the corresponding bonds in **5a** and **6a**. As a result, **3b** and **4a** exhibit a larger degree of bond length alternation in ring C than **5a** and **6a**. In connection with the greater bond

length alternation in ring C, the local aromaticity in **3b** and **4a** was evaluated quantitatively with the harmonic oscillator model of aromaticity (HOMA),²³ which is an aromaticity index of individual rings based on bond lengths.²⁴ A typical aromatic ring has a HOMA value of 1, and a smaller HOMA value indicates poorer aromaticity. As shown in Table 1, the HOMA values for ring C decrease from 0.773 in **5a** to 0.397 in **3b** and from 0.714 in **6a** to 0.339 in **4a**, respectively, indicating that the aromaticity of ring C in **5a** and **6a** is largely reduced upon fusing to the four-membered ring. This is also in agreement with calculated NICS values (Table S5 in ESI†).

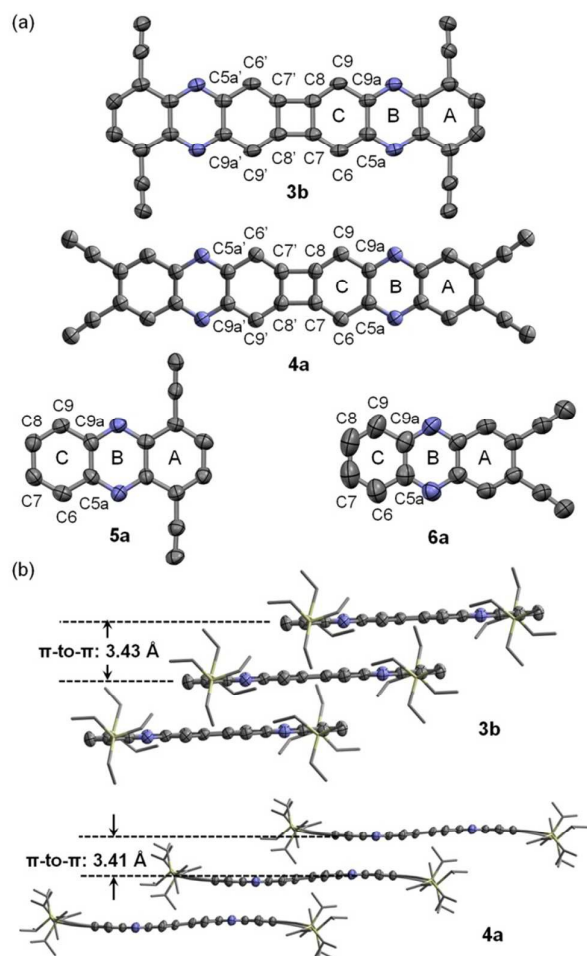


Fig. 2 (a) Molecular structures of **3b**, **4a**, **5a** and **6a** in single crystals with the trialkylsilyl substituents removed; (b) π -stacking of **3b** and **4a** in the crystals. (C and N atoms in (a) and in the polycyclic backbone in (b) are shown as ellipsoids at the 50% probability level; the trialkylsilylethynyl substituents in (b) are shown as sticks; hydrogen atoms are removed for clarity.)

As shown in Fig. 2b, molecules of **3b** in the crystals are arranged in one-dimensional π -stacks with a π -to- π distance of 3.43 Å. With a slightly bent π -backbone, molecules of **4a** form similar one-dimensional π -stacks with π -to- π distances of 3.41 Å (Fig. 2b) in the crystals. Despite similar one-dimensional π -stacks, **3b** exhibits a larger degree of π -overlap than **4a**. As shown in Fig. S4 (ESI†), two π -stacked molecules of **3b** have

more than four rings overlapped, while those of **4a** have only two rings overlapped. In comparison to **3b** and **4a**, phenazines **5a** and **6a** exhibit one-dimensional π -stacks with a head-to-tail arrangement of the silylethynyl substituents as shown in Fig. S5 in ESI†, likely as a result of substitution on only one side of these molecules. The π -to- π distances of **5a** and **6a** are 3.32 to 3.41 Å and 3.54 to 3.57 Å, respectively.

Table 1 Selected bond lengths and HOMA values of **3b**, **4a**, **5a** and **6a** from the crystal structures.

	3b	4a	5a	6a
C7–C8'	1.490(7)	1.494(5)	—	—
C7'–C8	1.490(7)	1.494(5)	—	—
C6–C7	1.345(6)	1.342(5)	1.372	1.341(2)
C7–C8	1.433(5)	1.443(3)	1.409	1.381(2)
C8–C9	1.345(6)	1.339(5)	1.366	1.352(2)
C9–C9a	1.443(6)	1.437(5)	1.408	1.415(2)
C5a–C9a	1.448(5)	1.445(3)	1.430	1.424(2)
C5a–C6	1.429(6)	1.435(5)	1.432	1.421(2)
HOMA	A	0.647	0.781	0.557
	B	0.795	0.821	0.802
	C	0.397	0.339	0.773

Table 2 Reduction potentials, absorption, emission, and frontier molecular orbital energy levels of **3a–6a**.

	Experimental					Calculated		
	E_{red}^1 (V) ^[a]	E_{red}^2 (V) ^[a]	LUMO (eV) ^[b]	λ_{max}^{Abs} (nm) ^[c]	λ_{max}^{Em} (nm) ^[d]	Φ_f (%) ^[e]	HOMO (eV) ^[f]	LUMO (eV) ^[f]
3a	-1.21	-1.54	-3.89	484	547	2.9	-6.04	-3.49
4a	-1.15	-1.49	-3.95	513	527	47.4	-6.29	-3.50
5a	-1.53	-2.09	-3.57	442	492	1.8	-6.03	-3.06
6a	-1.48	-2.10	-3.62	419	478	0.2	-6.33	-3.04

[a] Half-wave potential versus ferrocenium/ferrocene. [b] Estimated from LUMO = $-5.10 - E_{red}^1$ (eV).²⁵ [c] The longest-wavelength absorption maximum as measured from a 1×10^{-5} M solution in CH_2Cl_2 . [d] The shortest-wavelength emission maximum as measured from a 1×10^{-5} M solution in CH_2Cl_2 . [e] Fluorescence quantum yield. [f] Calculated at the B3LYP level of DFT with 6-311++G(d,p)//6-31G(d,p) basis sets using simplified model molecules (**3a'**, **4a'**, **5a'**, and **6a'**).

Photophysical properties and electronic structures

The most interesting aspect of CBDPs **3a–b** and **4a–b** is their electronic structures, which, in comparison to the corresponding phenazines, **5a** and **6a**, can shed light on the role of the four-membered ring in conjugation. To compare the electronic structures of CBDP and phenazine, **3a–6a** were studied with cyclic voltammetry (CV), UV-vis absorption spectroscopy, fluorescence spectroscopy, and density functional theory (DFT) calculations. In the test window of CV, **3a** and **4a** both exhibited two reversible reduction waves but did not exhibit any oxidation waves, while **5a** and **6a** both exhibited one reversible reduction wave and one quasireversible reduction wave with more negative reduction potentials than those of **3a** and **4a** (Fig. S6 in ESI†). The half-wave reduction potentials of **3a–6a** are shown in Table 2, and

ARTICLE

Journal Name

on the basis of the first reduction potentials versus ferrocenium/ferrocene, the LUMO energy levels are estimated as -3.89 eV for **3a**, -3.95 eV for **4a**, -3.57 eV for **5a**, and -3.62 eV for **6a**.²⁵

As shown in Fig. 3, the UV-vis absorption spectra of **3a** and **4a** exhibit apparent bathochromic shift relative to those of **5a** and **6a**, respectively, with much larger molar extinction coefficients (ϵ). The longest-wavelength absorption maximum of **3a** occurs at 484 nm ($\epsilon = 1.22 \times 10^5$ L·mol⁻¹·cm⁻¹), which is red-shifted by 42 nm relative to that of **5a**. The bathochromic shift of **4a** relative to **6a** is even larger, with the longest-wavelength absorption maximum of **4a** (513 nm, $\epsilon = 3.13 \times 10^5$ L·mol⁻¹·cm⁻¹) red-shifted by 94 nm relative to that of **6a**. The red shifts suggest considerable conjugation between the two phenazine subunits in **3a** and **4a**, and thus seem to contradict the bond lengths of the C7–C8' and C7'–C8 bonds in the crystal structures of **3b** and **4a**, which suggest very poor conjugation between the phenazine subunits in CBDPs. Such seeming contradiction can be reconciled by recognizing that the ground state and the electronically excited state may have different degree of conjugation.²⁶ The bond lengths in the crystal structures correspond to the ground-state geometry reflecting the conjugation in the ground state, while the UV-vis absorption, as a result of electronic transition from the ground state to the excited state, depends on the conjugation in both the ground and excited states. Considering the crystal structures are already indicative of very poor conjugation between the phenazine subunits in **3b** and **4a**, we conclude that the UV-vis absorption spectra of **3a** and **4a** are an indication of effective conjugation between the phenazine subunits in the excited state of CBDP. This conclusion is in agreement with the excited-state aromaticity of 1,3-cyclobutadiene and biphenylene, which is unfortunately not as well-known as the ground-state antiaromaticity of these compounds.²⁶

Upon irradiation with UV light, solution of **3a** in CH₂Cl₂ exhibited weak yellow fluorescence while solution of **4a** in CH₂Cl₂ exhibited strong green fluorescence as shown in Fig. 4. In comparison to **3a** and **4a**, phenazine **5a** in solution exhibited very weak blue fluorescence while **6a** in solution did not show visible fluorescence upon irradiation with UV light, in agreement with the well-known nonfluorescent property of nonsubstituted phenazine.²⁷ As detailed in ESI†, the fluorescence quantum yield (Φ_f) was measured as 0.03 for **3a**, 0.47 for **4a**, 0.02 for **5a** and 0.002 for **6a**.

To better understand the different photophysical properties of **3a** and **4a**, the frontier molecular orbitals of **3a–6a** were calculated using simplified model molecules **3a'–6a'**, which have smaller trimethylsilyl (TMS) groups replacing the TIPS groups to reduce computation cost. The geometries of these simplified molecules were optimized at the B3LYP level of DFT with the 6-31G(d,p) basis set, and the molecular orbitals were then calculated with the 6-311++G(d,p) basis set. As shown in Table 2, the calculated LUMO energy levels of **3a** and **4a** are lower than those of **5a** and **6a** by about 0.4 eV, respectively, while the calculated highest occupied molecular orbital (HOMO) energy levels of **3a** and **4a** are essentially the same as

those of **5a** and **6a**, respectively, in agreement with the UV-vis absorptions of **3a** and **4a** red shifted relative to those of **5a** and **6a**, respectively. Fig. 5 shows the selected molecular orbitals for **3a'** and **4a'**, which can be regarded as a result of combining the corresponding molecular orbitals of **5a'** and **6a'**, respectively, on the basis of the qualitative molecular orbital theory.²⁸ By comparing the molecular orbitals of **3a'** and **5a'**, particularly, in respect of the symmetry, it is found that the HOMO and HOMO–1 of **3a'** originate from the HOMO of **5a'**, and the LUMO and LUMO+1 of **3a'** originate from the LUMO of **5a'**. The LUMO and LUMO+1 of **3a'** exhibit larger splitting than the HOMO and HOMO–1 of **3a'**, suggesting that the two LUMOs of **5a'** are combined with stronger interactions than the two HOMOs of **5a'** in forming the corresponding molecular orbitals of **3a'**.²⁹ Furthermore, the LUMOs of **3a** and **4a** exhibit large

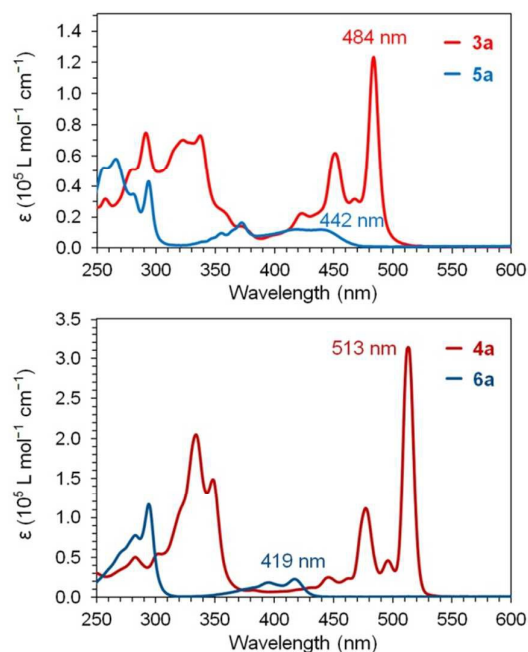


Fig. 3 UV-vis absorption spectra of **3a** versus **5a** (top) and **4a** versus **6a** (bottom) in CH₂Cl₂ at the same concentration (1×10^{-5} mol/L).

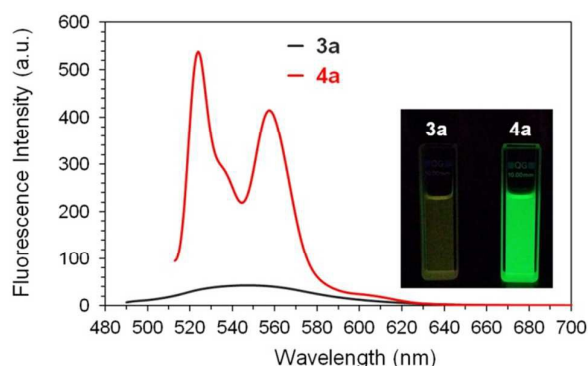


Fig. 4 Fluorescence spectra from solutions of **3a** and **4a** in CH₂Cl₂ (1×10^{-5} mol/L) when excited at 484 nm and 513 nm, respectively, and measured under the same condition. (Inset: photograph for luminescence of the above solutions of **3a** and **4a** upon irradiation with UV light at 365 nm.)

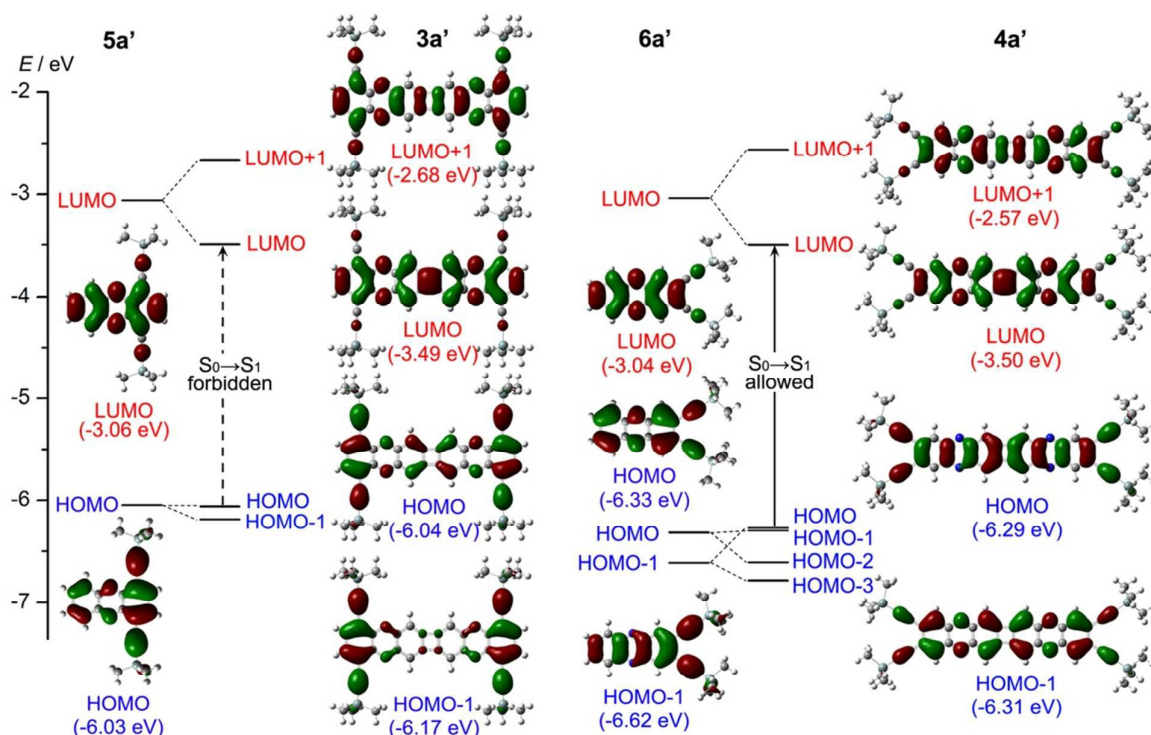


Fig. 5 Energy diagrams and the pictorial representations of the selected molecular orbitals for **3a'**–**6a'**.

coefficients on the four-membered ring with bonding interactions between C7 and C8' as well as C7' and C8.³⁰ These observations are in agreement with the conclusion that the two phenazine subunits in CDBP are poorly conjugated in the ground state but strongly conjugated in the excited state. Similarly, the LUMO and LUMO+1 of **4a'** originate from the LUMO of **6a'** with large splitting. In contrast, the HOMO and HOMO–1 of **4a'** with very close energy levels originate from different molecular orbitals of **6a'**. The HOMO and HOMO–3 of **4a'** originate from the HOMO–1 of **6a'**, while HOMO–1 and HOMO–2 of **4a'** originate from the HOMO of **6a'**. The HOMO–1 and HOMO–2 of **4a'** exhibit larger splitting than the HOMO and HOMO–1 of **3a'**, suggesting the two HOMOs of **6a'** interact more strongly than the two HOMOs of **5a'** in forming the corresponding molecular orbitals of **4a'** and **3a'**, respectively. Such different interactions may be attributed to the fact that the HOMO of **6a'** has higher density on C7 and C8 than that of **5a'**.³¹ Because of originating from the HOMO–1 of **6a'**, the HOMO of **4a'** has a symmetry (b_{2g}) different from that of **3a'** (a_u). As a result, the S_1 to S_0 transition of **4a'** ($B_{3u} \rightarrow A_g$) is symmetry-allowed according to the Laporte rule, in agreement with the high fluorescence quantum yield of **4a** ($\phi_f = 0.47$). In contrast, the S_1 to S_0 transition of **3a'** ($B_{1g} \rightarrow A_g$) is symmetry-forbidden in agreement with the low fluorescence quantum yield of **3a** ($\phi_f = 0.03$). Moreover, the symmetry-forbidden S_0 to S_1 transition of **3a** is not responsible to the longest-wavelength absorption of **3a** (Figure 4), which in fact can be attributed to the symmetry-allowed S_0 to S_2 transition ($A_g \rightarrow B_{2u}$) involving electronic excitation from HOMO–1 to

LUMO. The above results demonstrate that the electronic structure of CDBP can be largely tuned by adjusting the substituting positions of silylethynyl groups.

Thin film transistors

To test semiconductor properties of silylethynylated CDBPs, top-contact bottom-gate thin film transistors were fabricated by solution-based processes as detailed in ESI†. The solution-processed films of **3b** (Fig. 6a) and **4a** consisted of crystalline ribbons and fibers as found with a polarized-light microscope. The X-ray diffraction (XRD) from the film of **3b** exhibited a diffraction peak at $2\theta = 6.95^\circ$ (d spacing = 12.7 Å), which is in accordance with the (010) diffraction as derived from the crystal structure of **3b**. This indicates that molecules of **3b** adopt an edge-on orientation on the dielectric surface with an angle of 51.9° between the π -plane and the surface (Fig. S17 in ESI†). The XRD from the film of **4a** exhibited a diffraction peak at $2\theta = 5.28^\circ$ (d spacing = 16.7 Å), which do not correspond to any diffractions as derived from the crystal structure of **4a**, indicative of a thin film phase different from the single crystal phase. In contrast, dip coating or drop casting solutions of **3a** and **4b** under similar conditions resulted in tiny crystals that were not suitable for fabrication of thin film transistors likely related to their molecular packing in the solid state, which, however, remained unknown from crystal structures. As measured from at least 30 channels in vacuum, **3b** functioned as an n-type semiconductor with field effect mobility of 0.13 ± 0.05 cm²/Vs, which is higher than that of **1b** by one order of magnitude. The highest mobility of **3b** is 0.30 cm²/Vs, which is

extracted from the transfer I - V curve in the saturation regime as shown in Fig. 6b. Compound **4a** in the dip-coated films also functioned as an n-type semiconductor with field effect mobility of $0.019 \pm 0.007 \text{ cm}^2/\text{Vs}$, which is lower than that of **3b** by about one order of magnitude likely in relation to poorer π -overlap of **4a** in the solid state and the deep grain boundaries as found from the atomic force microscope (AFM) image (Fig. S13 in ESI[†]). In control experiments, thin films of **5a** and **6a** were also prepared by solution based process under similar conditions. Although both **5a** and **6a** were able to form continuous films containing crystalline fibers, deposition of top-contact electrodes by thermal evaporation of gold appeared problematic. The films of **5a** melt during deposition of gold because of the low melting point of **5a** (96–98 °C), while the crystalline fibers of **6a** cracked during this process. In the resulting transistors, **6a** functioned as an n-type semiconductor with low field effect mobility in the range of $10^{-4} \text{ cm}^2/\text{Vs}$, which can be attributed to its high LUMO energy level, the limited π -overlap in the solid state and the cracks in the films. On the other hand, thin films of **5a** and **6a** as dip coated on pre-fabricated bottom-contact gold electrodes did not exhibit any field effect presumably because of the poor contact between organic crystallites and the electrodes in these devices. The performance of **3b** and **4a** in comparison to that of **5a** and **6a** suggests that the four-membered ring is a useful linker to connect π -units for designing new n-type semiconductors. The field effect mobility of **3b** as reported here is still lower than that of the state-of-the-art solution-processed n-type organic semiconductors (i.e. $> 1 \text{ cm}^2/\text{Vs}$) by one order of magnitude.⁵ As suggested by the low-lying and fully delocalized LUMO and the large π -overlap in the solid state, **3b** may achieve higher electron mobility in thin film transistors if the quality of films could be improved by optimizing the conditions for device fabrication and the interface structures.

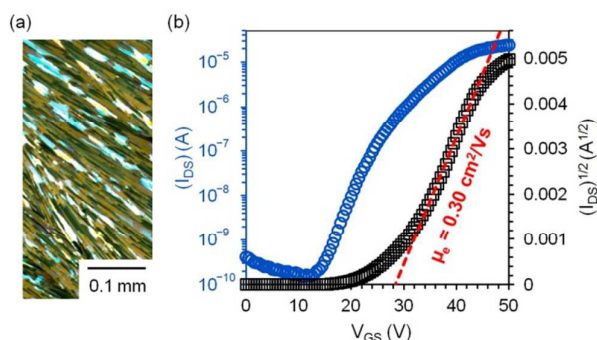


Fig. 6 (a) Reflection polarized light micrograph for a drop-casted film of **3b**; (b) drain current (I_{DS}) versus gate voltage (V_{GS}) with drain voltage (V_{DS}) at 50 V for an OTFT of **3b** with an active channel of $W = 1 \text{ mm}$ and $L = 50 \mu\text{m}$ as measured under vacuum.

Conclusions

In summary, this study puts forth a new π -electron molecular scaffold, CDBP, by connecting two phenazine moieties through

a four-membered ring. With properly positioned silylethynyl substituting groups, CDBP offers a chromophore with large molar extinction coefficients, a luminophore with good quantum yield, and an n-type organic semiconductor with field effect mobility as high as $0.30 \text{ cm}^2/\text{Vs}$. In contrast, these properties are not available with the phenazine reference compounds (**5a** and **6a**). This suggests that the four-membered ring is a versatile building block for designing novel π -electron systems for functional materials. On the basis of single crystal structures, UV-vis absorption and DFT calculation, we conclude that the two phenazine subunits in cyclobuta[1,2-b:3,4-b']diphenazine are poorly conjugated in the ground state but strongly conjugated in the excited state, shedding light on the role of the four-membered ring in conjugation.

Acknowledgements

We thank Ms. Hoi Shan Chan (the Chinese University of Hong Kong) for the single crystal crystallography. This work was supported by the Research Grants Council of Hong Kong (GRF 14300217) and the University Grants Committee of Hong Kong (project number: AoE/P-03/08).

Conflicts of interest

There are no conflicts to declare.

Notes and references

- O. Š. Miljanić and K. P. C. Vollhardt, in *Carbon-Rich Compounds*, (Eds.: Haley, M. M.; Tykwinski, R. R.), Wiley-VCH, Weinheim, 2006, Chapter 4.
- R. R. Parkhurst and T. M. Swager, *J. Am. Chem. Soc.*, 2012, **134**, 15351–15356.
- Z. Jin, Y. C. Teo, N. G. Zulaybar, M. D. Smith and Y. Xia, *J. Am. Chem. Soc.*, 2017, **139**, 1806–1809.
- A. Fukazawa, H. Oshima, S. Shimizu, N. Kobayashi and S. Yamaguchi, *J. Am. Chem. Soc.*, 2014, **136**, 8738–8745.
- a) B. Shan and Q. Miao, *Tetrahedron Lett.*, 2017, **58**, 1903–1911; b) K. Zhou, H. Dong, H. -L. Zhang and W. Hu, *Phys. Chem. Chem. Phys.*, 2014, **16**, 22448–22457.
- a) U. H. F. Bunz, *Acc. Chem. Res.*, 2015, **48**, 1676–1686; b) U. H. F. Bunz, J. U. Engelhart, B. D. Lindner and M. Schaffroth, *Angew. Chem., Int. Ed.*, 2013, **52**, 3810–3821; c) J. Li, Q. Zhang, *ACS Appl. Mater. Interfaces*, 2015, **7**, 28049–28062.
- a) Q. Miao, *Synlett*, 2012, **23**, 326–336; b) Q. Miao, *Adv. Mater.*, 2014, **26**, 5541–5549.
- P. Biegger, M. Schaffroth, C. Patze, O. Tverskoy, F. Rominger and U. H. F. Bunz, *Chem.—Eur. J.*, 2015, **21**, 7048–7052.
- P. Biegger, M. Schaffroth, O. Tverskoy, F. Rominger and U. H. F. Bunz, *Chem.—Eur. J.*, 2016, **22**, 15896–15901.
- S. Yang, B. Shan, X. Xu and Q. Miao, *Chem.—Eur. J.*, 2016, **22**, 6637–6642.

- 11 a) F. Paul, J. Patt and J. F. Hartwig, *J. Am. Chem. Soc.*, 1994, **116**, 5969–5970; b) A. S. Guram and S. L. Buchwald, *J. Am. Chem. Soc.*, 1994, **116**, 7901–7902.
- 12 B. D. Lindner, J. U. M. Märken, O. Tverskoy, A. L. Appleton, F. Rominger, K. I. Hardcastle, M. Enders and U. H. F. Bunz, *Chem.—Eur. J.*, 2012, **18**, 4627–4633.
- 13 T. A. Albright, S. Oldenhof, O. A. Oloba, R. Padilla and K. P. C. Vollhardt, *Chem. Commun.*, 2011, **47**, 9039–9041.
- 14 a) W. J. Youngblood, *J. Org. Chem.* 2006, **71**, 3345–3356; b) J. Wang and L. Wang, CN1887851, 2007.
- 15 J. D. Spence, A. C. Rios, M. A. Frost, C. D. McCutcheon, C. M. Cox, S. Chavez, R. Fernandez and B. F. Gherman, *J. Org. Chem.*, 2012, **77**, 10329–10339.
- 16 V. R. Thalladi, T. Smolka, A. Gehrke, R. Boese and R. Sustmann, *New J. Chem.*, 2000, **24**, 143–147.
- 17 J. J. Bryant, Y. Zhang, B. D. Lindner, E. A. Davey, A. L. Appleton, X. Qian and U. H. F. Bunz, *J. Org. Chem.*, 2012, **77**, 7479–7486.
- 18 CCDC 1570598, 1570599 and 1570601 contain the supplementary crystallographic data for **3b**, **4a** and **6a**, respectively. These data can be obtained free of charge from the Cambridge Crystallographic Data Centre via www.ccdc.cam.ac.uk/data_request/cif.
- 19 P. Biegger, S. Stolz, S. N. Intorp, Y. Zhang, J. U. Engelhart, F. Rominger, K. I. Hardcastle, U. Lemmer, X. Qian, M. Hamburger and U. H. F. Bunz, *J. Org. Chem.*, 2015, **80**, 582–589.
- 20 J. K. Fawcett and J. Trotter, *Acta Crystallogr.*, 1966, **20**, 87–93.
- 21 E. V. Anslyn and D. A. Dougherty, *Modern Physical Organic Chemistry*, University Science Books, Sausalito, 2004, ch. 1, pp. 22.
- 22 A. Schleifenbaum, N. Feeder and K. P. C. Vollhardt, *Tetrahedron Lett.*, 2001, **42**, 7329–7332.
- 23 a) J. Kruszewski and T. M. Krygowski, *Tetrahedron Lett.*, 1972, 3839–3842; b) T. M. Krygowski *J. Chem. Inf. Comput. Sci.*, 1993, **33**, 70–78.
- 24 HOMA is a quantitative measure of aromaticity based on bond length as defined by
- $$\text{HOMA} = 1 - \frac{\alpha^{CC}}{n} \sum (R_{opt}^{CC} - R_i^{CC})^2 \text{ for a carbocycle, or}$$
- $$\text{HOMA} = 1 - \frac{1}{n} \left\{ \alpha^{CC} \sum (R_{opt}^{CC} - R_i^{CC})^2 + \alpha^{CN} \sum (R_{opt}^{CN} - R_i^{CN})^2 \right\}$$
- for a N-heterocycle, where n is the number of bonds taken into the summation, $\alpha^{CC} = 257.7$ and $\alpha^{CN} = 93.52$ are empirical normalization constants chosen to give HOMA = 0 for the hypothetical Kekulé structures of the typical aromatic systems with alternation of single and double bonds and HOMA = 1 for the system with all bond lengths equal to the optimal value R_{opt} (1.388 Å for C-C bonds and 1.334 Å for C-N bonds), and R_i is the individual bond length in the ring. See: T. M. Krygowski and M. K. Cyrański, *Chem. Rev.*, 2001, **101**, 1385–1419.
- 25 The commonly used formal potential of the redox couple of ferrocenium/ferrocene (Fc^+/Fc) in the Fermi scale is -5.1 eV, which is obtained on the basis of an approximation neglecting solvent effects with a formal potential of -4.46 eV for the normal hydrogen electrode (NHE) in the vacuum scale and an electrochemical potential of 0.64 V for Fc^+/Fc versus NHE. See: C. M. Cardona, W. Li, A. E. Kaifer, D. Stockdale and G. C. Bazan, *Adv. Mater.*, 2011, **23**, 2367–2371.
- 26 M. Rosenberg, C. Dahlstrand, K. Kilsa and H. Ottosson, *Chem. Rev.*, 2014, **114**, 5379–5425.
- 27 A. Grabowska and B. Paluła, *Photochem. Photobiol.*, 1969, **9**, 339–350.
- 28 E. V. Anslyn and D. A. Dougherty, *Modern Physical Organic Chemistry*, University Science Books, Sausalito, 2004, ch. 1, pp. 26–51.
- 29 C. D. Cruz, P. R. Christensen, E. L. Chronister, D. Casanova, M. O. Wolf and C. J. Bardeen, *J. Am. Chem. Soc.*, 2015, **137**, 12552–12564.
- 30 B. Milián-Medina and J. Gierschner, *WIREs Comput Mol Sci*, 2012, **2**, 513–524.
- 31 a) T. Higashino, T. Yamada, T. Sakurai, S. Seki and H. Imahori, *Angew. Chem. Int. Ed.*, 2016, **55**, 12311–12315; b) Y. Yamaguchi, K. Ogawa, K. Nakayama, Y. Ohba and H. Katagiri, *J. Am. Chem. Soc.*, 2013, **135**, 19095–19098.

This study puts forth cyclobuta[1,2-b:3,4-b']diphenazine (CBDP), a new π -electron molecular scaffold containing two phenazine moieties connected by a four-membered ring. CBDP exhibits interesting optical and electronic properties that can be tuned by adjusting the substituting positions of silylethynyl groups but are not offered by the phenazine reference compounds, leading to solution-processed n-type semiconductors with field effect mobility of up to $0.30 \text{ cm}^2/\text{Vs}$.

